

QUT Digital Repository:  
<http://eprints.qut.edu.au/>



This is the submitted version of the following journal article:

[Ke, Xuebin](#), [Zhu, Huai Yong](#), [Gao, Xueping](#), [Liu, Jiang-Wen](#), & [Zheng, Zhanfeng](#) (2007) High-performance ceramic membranes with a separation layer of metal oxide nanofibers. *Advanced Materials*, 19(6), pp. 785-790.

© Copyright 2007 WILEY-VCH Verlag GmbH & Co. KGaA, Weinheim

# High-Performance Ceramic Membranes with a Separation Layer of Metal Oxide Nanofibers

Xue Bin Ke<sup>1</sup>, Huai Yong Zhu<sup>1\*</sup>, Xue Ping Gao<sup>2\*</sup>, Jiang Wen Liu<sup>1</sup>, Zhan Feng Zheng<sup>1</sup>

<sup>1</sup> School of Physical and Chemical Sciences, Queensland University of Technology, Brisbane, Qld 4001, Australia, <sup>2</sup> Institute of New Energy Material Chemistry, Nankai University, Tianjin 300071, China.

\* To whom correspondence should be addressed. Email: [hy.zhu@qut.edu.au](mailto:hy.zhu@qut.edu.au) (H.Y.Z.); [xpgao@nankai.edu.cn](mailto:xpgao@nankai.edu.cn) (X.P.G.).

Ceramic separation membranes are of particular interest in many separation processes because they can be used under severe conditions due to their chemical and thermal stability<sup>[1-3]</sup>. They are able to function unaffected within organic and biological systems and at high temperatures, can be readily cleaned (or sterilised) by steam-treatment, and exhibit long operational lives. The low energy consumption and absence of potentially harmful chemical agents within the separation processes using ceramic membranes for both gases and liquids also presents additional economic and social imperatives<sup>[2-3]</sup>. These outstanding and compelling features have resulted in the rapid adaptation of ceramic membranes within the dairy, food, pharmaceutical, bioengineering, chemical, nuclear energy, water-treatment and electronic industries<sup>[1-6]</sup>. The porous ceramic membranes have an unsymmetrical layered structure, consisting of a macroporous (pore size > 400 nm) support, a porous intermediate-layer and a nanoporous top-layer<sup>[1-6]</sup>. The support and layers are usually made of oxide particles with the voids between the particles forming passageways through the membrane (i.e.,

continuous porosity), which are used for filtration. The thick macroporous support (of up to several millimetres) provides the necessary mechanical strength of the membrane. The intermediate-layer usually is applied to the macroporous support next to prevent the small particles used for forming the top-layer from blocking the micropores in the support. Such blocking can substantially reduce the flux through the membrane [2]. The top-layer usually is applied to the intermediate-layer macroporous support using sols of metal hydrates [1-6]. The sols are applied layer by layer in a sequence of decreasing size of the sol particles to achieve inter-particle voids which are effective for separation. The selectivity of the membrane is controlled solely by the pore size of the top-layer, and the flux passing through the filter depends, predominantly, on the thickness of the top-layer. Therefore, the top-layer fulfils the actual separation function of the membrane. However, the top-layers of the ceramic membranes fabricated under the conventional approaches are aggregates of particles in nature, and are unable to permit a high flux while maintaining good selectivity. In addition, the conventional approach encounters significant difficulties due to the formation of pin-holes and cracks during the drying and calcination process, and a dramatic loss of flux when pore sizes are reduced to increase selectivity [6-14].

To pursue ceramic membranes with high efficiency, we have to introduce radical changes in the membrane texture because the membrane texture is crucial to the separation efficiency and should be of primary concern when developing separation membranes. In the present study, we constructed ceramic nanofilters with a hierarchically structured separation layer on a porous substrate using larger titanate and smaller boehmite nanofibers. The randomly oriented titanate nanofibers can completely cover the rough surface of the porous substrate of  $\alpha$ -alumina particles with a size of

several microns, leaving no pin-holes and cracks. On the top of this titanate fiber layer a layer of  $\gamma$ -alumina fibers were formed using boehmite (AlOOH) nanofibers. The resulting membranes can effectively filter out species larger than 60 nm at flow rates orders of magnitude greater than conventional membranes, and are immune to the structural deficiencies in the conventional ceramic membranes. The use of ceramic nanofibers or nanorods, instead of particulates with irregular shapes, to fabricate ceramic membranes is a new direction in developing high performance ceramic membranes.

The mesh structure of threads should be the most efficient structure for filtration, which achieves high selectivity and maintains much higher flux in comparison to membranes of other forms. Recently, electro-spinning process has been employed to produce polymeric fibers with diameters less than 100 nm, and the obtained fibers could potentially be used for fabricating highly ordered membrane architectures <sup>[11-14]</sup>, although high flux rate has not yet been achieved.

On the other hand, nanorods or nanofibers of various metal oxides and hydrous oxides, including copper oxide <sup>[15]</sup>, alumina <sup>[16, 17]</sup>, silica <sup>[18]</sup>, titanate <sup>[19]</sup> and rare earth oxides <sup>[20]</sup> have been synthesized recently. The dimension of these nanorods or nanofibers resides within a wide range. For instance, by adjusting the synthesis conditions we can tailor the thickness of boehmite (AlOOH) fibers from 3 to 10 nm and length from 40 to 100 nm <sup>[17]</sup>, and tailor the thickness of the titanate fibers from 10 nm to 100 nm and the length from 100 nm to 20-30  $\mu$  <sup>[19]</sup>. These inorganic nanofibers could be readily dispersed in aqueous or alcohol solutions. This allows us to construct layers of randomly oriented fibers (LROF) on a porous ceramic substrate as the separation layer by applying thin layers of the dispersed nanofibers. Furthermore, we can construct

hierarchical LROF structures, in which the layers of the smaller fibers lay on the top of the layers of larger fibers, so that the selectivity of the membranes can be controlled within a wide range. The resulting membranes with such a structure should possess the merits of ceramic membranes, being able to withstand steam cleaning and regeneration at high temperatures. These properties are crucial for the applications of the ceramic membranes [3].

The minimum pore size for the filtration in the web structures is the thickness of the fibers used to constructing the web. Therefore, it is possible to construct the LROF structures which are able to filtrate out the species with a size of tens of nanometers with the reported metal oxide fibers. Membranes which have the ability to filter out species larger than 50-60 nm have attracted significant interest due to the variety of important applications they are able to perform [7-14]. For example, most viruses and waterborne pathogens are larger than 50-60 nm. The two viruses that are currently of major concern to the international community are the Severe Acute Respiratory Syndrome (SARS) corona virus which is 80-200 nm in size and the avian flu virus which is 80-120 nm in diameter [2-3, 21-25]. Such membranes are able to effectively filter out these dangerous viruses within the air, water and even the blood [7-14]. Double-layered nanoporous membrane with cylindrical pores has already been successfully documented in virus filtration [8]. It exhibits high sensitivity and flux for the separation of the human pathogen of the common cold in humans. Kang and Shah reported microporous polypropylene membrane filters modified with a cationic surfactant for separating particles of about 60 nm [9]. The modification increased the capture efficiency from 10% to 95%. Researchers of Pacific Northwest National Laboratory used self-assembled monolayers on mesoporous supports to accurately control pore sizes [7].

These membranes also have great industrial potential for separation processes within the dairy, food, pharmaceutical, petrochemical and radioactive material processing industries. In these applications, the stability of ceramic membranes is a desired merit: the membranes can be cleaned readily with steam, and have long operation life and no risk of causing contamination.

To verify the concept of LROF structure as the top-layer for ceramic membranes, we have constructed for the first time ceramic membranes with a hierarchical LROF structure using nanofibers of boehmite and titanate, for the separation of the species larger than 60 nm. The boehmite nanofibers, which can be converted to  $\gamma$ -alumina fibers through heating at temperature above 773 K <sup>[16, 17]</sup>, and titanate nanofibers <sup>[19]</sup> were used for making the web-structures. The scanning electron microscopy (SEM) image of the alumina substrate and transmission electron microscopy (TEM) images of the nanofibers are shown in Fig. 1.

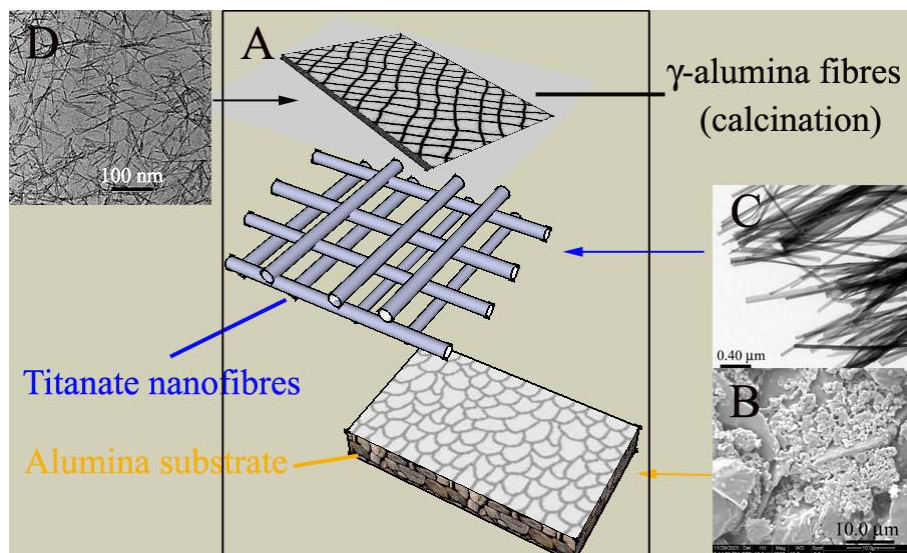


**Figure 1** The components of hierarchical LROF structure. (A) Schematic profiles of the ceramic membranes with LROF structures of titanate and  $\gamma$ -alumina nanofibers. (B) A SEM micrograph of the  $\alpha$ -alumina substrate surface.

**(C) A TEM image of the titanate nanofibers. (D) A TEM image of the boehmite nanofibers, which will convert into  $\gamma$ -alumina nanofibers when being heated at 773 K.**

The substrate consists of small (2-3  $\mu$ ) and large (over 10  $\mu$ )  $\alpha$ -alumina particles, and the substrate surface is considerably rough. The porosity of the substrate is about 30-40%. The titanate fibers are 20-30  $\mu$  long and 40-100 nm thick (Fig. 1C), the small boehmite fibers with 60-100 nm long and 2-5 nm thick (Fig. 1D).

The titanate fibers were dispersed into ethanol, forming a suspension. The suspension was sonicated using an ultrasonic finger for 10 min to achieve a homogeneous dispersion which then was applied in layers on the  $\alpha$ -alumina substrate using a spin-coater. As illustrated in Fig. 1A and Fig. 2, after three consecutive coatings with the dispersion, the titanate nanofibers are lying down randomly on the substrate, covering the entire rough surface. The coating parameters such as content of fibers and number of coatings can be optimized according to the porous substrate. Generally, a very rough substrate surface, as the illustrated in Fig. 1B, can be covered sufficiently by applying 0.2 wt% dispersion several times. This eliminated the need for intermediate-layer and smooth substrate surfaces, which has been a costly manufacturing prerequisite under the conventional method, allowing this approach to be used for various substrates directly in order to achieve significant cost efficiencies in membrane fabrication. More importantly, there are no pin-hole and cracks after multiple coatings with the dispersion of nanofibers and subsequent calcinations (Fig. 2B and 2C). This ensures more successful and cost effective large scale fabrications by eliminatig lost production due to cracks and pin holes.

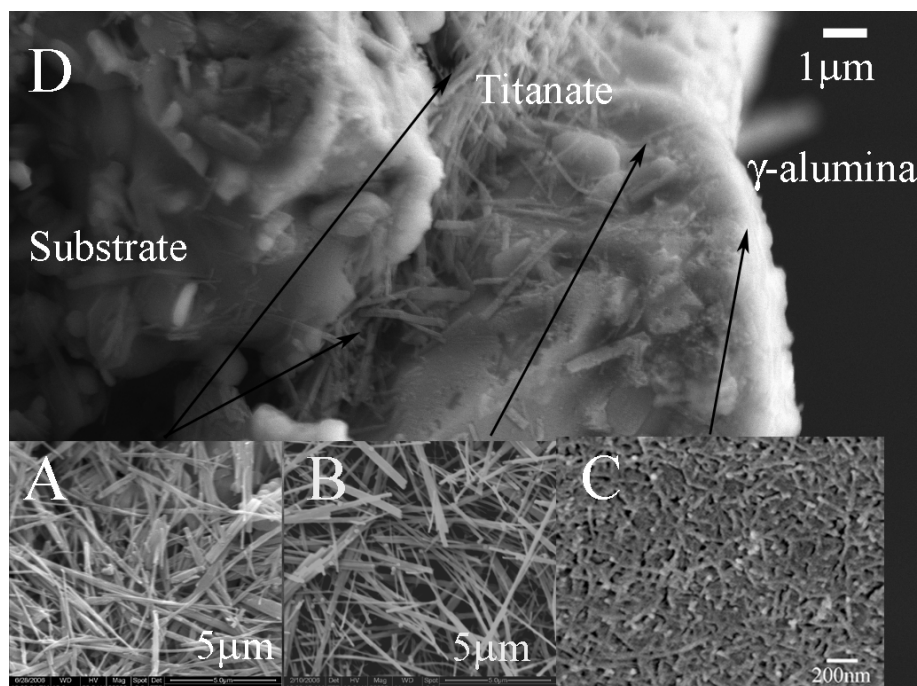


**Figure 2** The construction of the LROF structure. (A) A SEM micrograph of the LROF membrane surface on the  $\alpha$ -alumina substrate after the first coating with 0.2 wt% of titanate fiber dispersion. (B) A SEM micrograph of the membrane surface after the third coating with 0.2 wt% of titanate fiber dispersion. (C) A SEM micrograph of the LROF membrane surface after the coating with 0.2 wt% of boehmite fiber dispersion on the top of the LROF formed by three coatings of titanate fiber dispersion and the subsequent calcinations at 773 K. The  $\gamma$ -alumina fibers appear thicker because of the gold sputtering during the preparation of specimen for the SEM. (D) The cross section of the membrane shown in image (C).

The pore size of the  $\alpha$ -alumina substrate is up to ten microns, and the LROF structure of titanate fibers, formed by the spin-coating, has pore sizes of 100-200 nm. Further reduction in pore size to tens of nanometers with these titanate fibers becomes difficult. Nonetheless, the layer of randomly oriented titanate nanofibers can serve as substrate on which we applied coatings of the boehmite nanofibers to form the LROF



structure of smaller pores because the boehmite nanofibers are thinner and shorter than the titanate fibers. The homogeneous dispersion of boehmite nanofibers, used for the spin-coating, was prepared similarly by dispersing boehmite nanofibers into ethanol solution. The boehmite fibers can then be converted to  $\gamma$ -alumina nanofibers by calcination at 773 K for 2 h <sup>[16]</sup>. The morphology of alumina nanofibers remains similar to the parent boehmite nanofibers so that a LROF structure of alumina fibers, with smaller filtration pores, forms on the frame of titanate nanofibers (Fig. 2C). Such a hierarchical structure of LROF structures with decreasing pore sizes further enhances the selectivity of the membrane.

The filtration property of the membrane with the LROF structure was tested by filtering latex spheres in aqueous dispersion. The concentration of the latex sphere dispersion was 0.01 wt%, and spheres of different sizes were used. 30 mL of the dilution was tested to permeate the prepared membrane. To drive the flux through the membrane, a vacuum was introduced to the permeated fluid to keep a stable pressure difference between the feeding and the permeated fluids at 20 kPa. The concentrations of the latex spheres in the original dispersion and filtrate were determined by two techniques: SEM and UV-Vis spectroscopy <sup>[9, 26-27]</sup>. 5  $\mu$ L of solution was taken to prepare SEM specimen. The SEM images of the latex dispersion and its filtrate are shown in Fig. 3. By comparing these images we are able estimate the separation properties of the LROF structures.

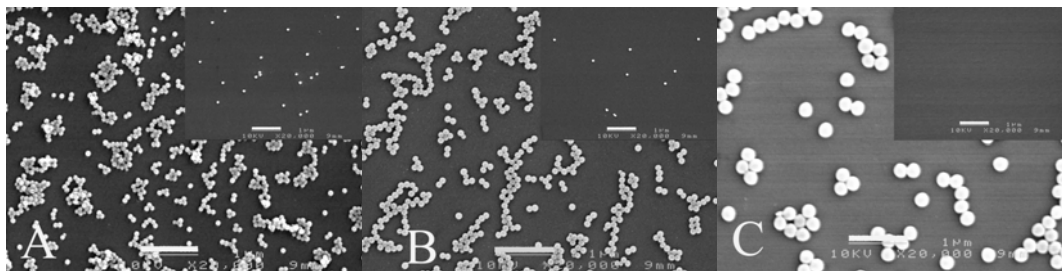


**Figure 3** SEM micrographs of the specimens taken from the feeding and the permeated (insert) fluids in filtrations of the solutions of Latex spheres with different sizes: (A) 60 nm, (B) 108 nm and (C) 200 nm. Scale bars in the images indicate the length of 1  $\mu\text{m}$ . The membrane after three coatings of  $\gamma$ -alumina fibers on top of the coatings of titanate fibers can filter out 96.8 % of latex spheres of 60 nm, 98.2 % the spheres of 108 nm and 100% of the sphere of 200 nm.

The LROF structure formed after three coating with titanate nanofibers can filtrate out 100 % of the latex spheres of 200 nm (Fig. 3). This membrane is able to retain a flux rate between 800 and 1000  $\text{L}/\text{m}^2\cdot\text{h}$ , which is over 2/3 of that of the alumina substrate (more than 1200  $\text{L}/\text{m}^2\cdot\text{h}$ ).

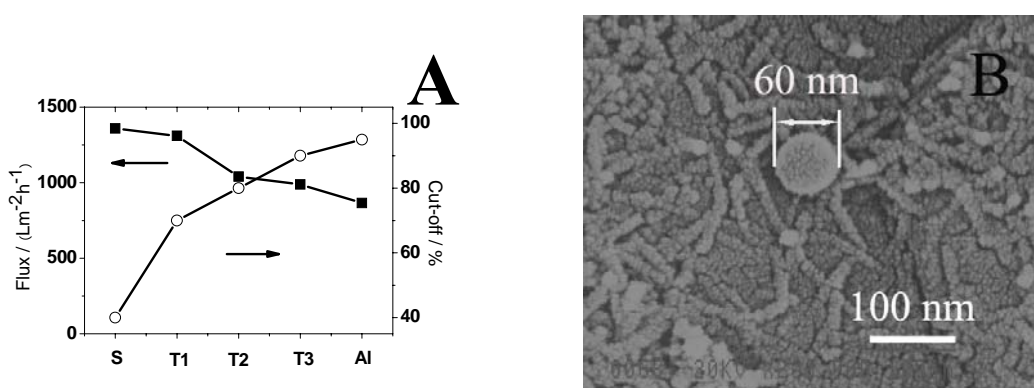


**Figure 4** The filtration property of the membranes with the LROF structure. (A) Filtration flux and selectivity of various membranes for filtering a 0.01 wt%

**solution of 60 nm Latex spheres (S is for the  $\alpha$ -alumina substrate; T1 is for the membrane after the first coating with titanate fibers, T2 is for that after the second coating with titanate fibers, T3 is that after the third coating with titanate fibers, A1 is for that after three coatings of  $\gamma$ -alumina fibers on top of the coatings of titanate fibers). (B) Surfaces of a membrane with the LROF structure (A1 in panel A) after the filtering. A 60 nm Latex sphere can be seen.**

The membrane with a layer of randomly oriented titanate nanofibers (three coatings) and a layer of randomly oriented alumina nanofibers (three coatings) are able to filter out 96.8 % of latex spheres with the size of 60 nm, while maintaining a relative high flux rate between 600 and 900 L/m<sup>2</sup>·h, which is 70-80% of the membranes with the meshes of titanate fibers only and over ½ of that for the alumina substrate. Such a flux rate is significantly greater than the flux rate of the membranes prepared under conventional approaches which exhibited similar separation. For instance, it is over 100 times greater than the rate reported in reference 3, and over 15 times greater than the rate in latest report [8]. The high flux is an outstanding advantage for the separations in liquid phase [28]. We also prepared a  $\gamma$ -alumina membrane by conventional method [29]. When the membrane is able to filter out above 95.0 % of latex spheres of 60 nm, its flux rate is 76 Lm<sup>-2</sup>·h<sup>-1</sup>, being about one tenth of the LROF membranes.

The high flux of the LROF structure comes from its large porosity. The filtration passages are voids in the separation layer. When the size of the voids are similar (means a similar selectivity of the separation layer), the flux passing through the membrane increases with the volume of the voids. For the ideal and simplest texture, a mesh made of nanofibers with a thickness of 10 nm and has a uniform pore size of 60 nm, the

porosity is over 73.5%. Such a mesh texture is similar to that shown in Figure 1A for the LROF structure of titanate nanofibers, but with a smaller dimension. The porosity does not change substantially even if the fibers are arranged randomly rather than forming a regular mesh. In contrast, the porosity of random packed metal oxide spherical particles in ceramic membranes is 36% or below <sup>[28]</sup>. To determine the pore structure of the separation layer of titanate and  $\gamma$ -alumina fibers, a film with three coatings of  $\gamma$ -alumina fibers on top of three coatings of titanate fibers was prepared on a quartz slide in the same procedures as for the LROF membrane. This film should possess the similar pore structure as the LROF membrane on the alumina support. The BET specific surface area of the LROF membrane is 35.5 m<sup>2</sup>/g, being slightly larger than that of the titanate fibers (about 30 m<sup>2</sup>/g). Given that the BET surface area of the  $\gamma$ -alumina nanofibers after calcination at 773K is over 370 m<sup>2</sup>/g, <sup>[16]</sup> the result indicates that  $\gamma$ -alumina nanofibers account a small fraction of the mass in the membranes, and the layer of the alumina fibers is thin. The pore size distribution (PSD) is derived from the nitrogen adsorption data of the film (Fig. S1 in Supporting materials). The results show that most of the porosity of the film comes from the pores larger than 10 nm and these pores are passages for the filtration. In contrast, a  $\gamma$ -alumina film prepared in the same procedures as for the  $\gamma$ -alumina membrane <sup>[29]</sup> has most of its porosity from the pores about 3 nm but a small quantity of pores above 10 nm (Fig. S1). The large pore sizes of the LROF membranes explain their high flux rates.

The nanofibers in the LROF structure can more effectively divide a space to small voids and occupy relative smaller space, compared to packed spherical nanoparticles, enabling the LROF structure to be much more efficient than the conventional top and intermediate layers of aggregated particles.

The calcination after spin-coating creates solid linkages between the fibers and between fibers and substrate, in addition to convert boehmite into  $\gamma$ -alumina nanofibers. The titanate fibers maintain fibril morphology up to 973 K <sup>[19]</sup>, and no other phase was observed, apart from the  $\alpha$ - and  $\gamma$ -alumina and titanate, according to the x-ray diffraction pattern (Figure S2 in Supporting Information). It is most likely that the hydroxyl groups from different fibers or from a fiber and the substrate condense in the contacting areas. It results in formation bonds between the fibers and between the fibers and the substrate, and yields water molecules. The LROF structures are bonded together and with the substrate after the calcination. To examine the stability of the LROF structures, we repeated 6 runs of filtration test and a calcination at 773K with a LROF membrane. The selectivity of the membrane after each calcination is above 95% and the flux varied between 700 and 860 L/m<sup>2</sup>·h<sup>-1</sup>, no obvious deterioration on either selectivity or flux has been observed. Therefore, the membranes with a top-layer of LROF structures can be used repeatedly and can be regenerated easily by heating. Another advantage of the LROF structures of nanofibers is that the sintering which often causes deterioration of selectivity and flux rate is much less for fibers than for particles <sup>[16]</sup>. The sintering of particles always commences from the contacting areas of particles. The contacting areas between fibers are smaller, compared with that between particles of other morphologies.

Additional benefits of using titanate nanofibers are also due to their high compatibility with biological substances, because of their non-toxicity, their ability to withstand dissolution in water and photostability<sup>[30]</sup>. The use of alumina fibers is due to their ability to attract and retain electronegative particles such as virus and bacteria<sup>[10]</sup>.

This widens the potential applications of the mesh membranes in its ability to deal with biological substances.

This study clearly demonstrates that the separation efficiency of ceramic membranes can be significantly improved through radical changes in the texture of the top-layer. The ceramic membranes with a hierarchical LROF structure as the separation layer exhibit both very high flux rate and excellent selectivity. Moreover, such a LROF structure is inherently “immune” to cracks, pin-hole and serious sintering. It enables this approach to be more successfully scaled-up for fabrication of ceramic membranes. The concept and the approach of constructing a hierarchical LROF structure as separation layer provide new opportunities in developing the next generation of ceramic membranes with high flux. Besides, as illustrated in the Experimental Section, the fabrication of these membranes offer a much more simplistic and economically efficient method of production, compared to the conventional ceramic membrane fabrication process. We are also able to tailor the selectivity of the membranes by choosing fibers which meet the requirement of various applications. This also allows us to further functionalize membranes, for instance, making membranes active for photocatalytically decomposing organic pollutants, viruses and bacteria by forming anatase crystals on the surface of titanate fibers <sup>[19]</sup>.

### **Acknowledgements**

This work is supported by the Australian Research Council (ARC) and the NSFC (90206043) of China.

### **References and Notes**

- [1] R. M. de Vos, H. Verweij, *Science* **1998**, 279, 1710.
- [2] H. Verweij, *J. Mater. Sci.* **2003**, 38, 4677.

- [3] L. Cot, A. Ayrat, J. Durand, C. Guizard, N. Hovnanian, A. Julbe, *Solid State Sci.* **2000**, *2*, 313.
- [4] A. I. Schäfer, A. G. Fane, T. D. Waite, *Nanofiltration-principles and applications*, Elsevier, Oxford **2003**.
- [5] S. P. Nunes, M. L. Sforça, K. Peinemann, *J. Membrane. Sci.* **1995**, *106*, 49.
- [6] a) R. W. Baker, *Membrane Technology and Applications*, 2<sup>nd</sup> ed, Wiley, West Sussex **2004**. b) R. R. Bhave, *Inorganic Membranes: Synthesis, Characterisation and Applications*, New York, Van Norstrand Reinhold, **1991**.
- [7] T. Harper, C. R. Vas, P. Holister, *Chem. Eng. Prog.* **2003**, *99*, 34.
- [8] S. Y. Yang, I. Ryu, H. Y. Kim, J. K. Kim, S. K. Jang, T. P. Russell, *Adv. Mater.* **2006**, *18*, 709.
- [9] P. K. Kang, D. O. Shah, *Langmuir* **1997**, *13*, 1820.
- [10] Tepper, F., Rivkin, T. *Filtr. Separat.* **2002**, *39*, 16.
- [11] M. G. Mckee, J. M. Layman, M. P. Cashion, T. E. Long, *Science* **2006**, *311*, 353.
- [12] A. G. Macdiarmid, *Angew. Chem., Int. Ed.* **2001**, *40*, 2581.
- [13] P. Katta, M. Alessandro, R. D. Ramsier, G. G. Chase, *Nano Lett.* **2004**, *4*, 2215.
- [14] D.H. Sun, C. Chang, S. Li, L. Lin, *Nano Lett.* **2006**, *6*, 839.
- [15] X. P. Gao, J. L. Bao, G. L. Pan, H. Y. Zhu, F. Wu, D. Y. Song, *J. Phys. Chem. B* **2004**, *108*, 5547.
- [16] H. Y. Zhu, J. D. Riches, J. C. Barry, *Chem. Mater.* **2002**, *14*, 2086.
- [17] H. Y. Zhu, X. P. Gao, D. Y. Song, Y. Q. Bai, S. P. Ringer, Z. Gao, Y. X. Xi, W. Martens, J. D. Riches, R. L. Frost, *J. Phys. Chem. B* **2004**, *108*, 4245.
- [18] a) J. Wang, J. Zhang, B. Y. Asoo, G. D. Stucky, *J. Am. Chem. Soc.* **2003**, *125*, 13966. b) J. Wang, C. K. Tsung, R. C. Hayward, Y. Wu, G. D. Stucky, *Angew. Chem., Int. Ed.* **2005**, *44*, 332. c) B. Wang, C. Chi, W. Shan, Y. Zhang, N. Ren, W. Yang, Y. Tang, *Angew. Chem., Int. Ed.* **2006**, *45*, 2088.
- [19] a) H. Y. Zhu, X. P. Gao, Y. Lan, D. Y. Song, Y. X. Xi, J. C. Zhao, *J. Am. Chem. Soc.* **2004**, *126*, 8380. b) H. Y. Zhu, Y. Lan, X. P. Gao, S. P. Ringer, Z. F. Zheng, D. Y. Song, J. C. Zhao, *J. Am. Chem. Soc.* **2005**, *127*, 6730.
- [20] P. X. Huang, F. Wu, B. L. Zhu, X. P. Gao, H. Y. Zhu, T. Y. Yan, W. P. Huang, S. H. Wu, D. Y. Song, *J. Phys. Chem. B* **2005**, *109*, 19169.
- [21] a) P. R. Murray, K. S. Rosenthal, M. A Pfaller, *Medical Microbiology*, 5<sup>th</sup> ed., Elsevier Mosby, Philadelphia, **2005**. b) L. Fiksdal, T. Leiknes, *J. Membr. Sci.* **2006**, *279*, 364.
- [22] Y. Lin, X. Yan, W. Cao, C. Wang, J. Feng, J. Duan, S. Xie, *Antiviral Ther.* **2004**, *9*, 287.
- [23] T. G. Ksiazek et al., *New Engl. J. Med.* **2003**, *348*, 1953.
- [24] R. J Webby, R. G. Webster, *Science* **2003**, *302*, 1519.
- [25] T. Noda, H. Sagara, A. Yen, A. Takada, H. Kida, R. H. Cheng, Y. Kawaoka, *Nature* **2006**, *439*, 490.
- [26] A. Akthakul, A. I. Hoxhbaum, F. Stellacci, A. M. Mayes, *Adv. Mater.* **2005**, *17*, 532.
- [27] T. Leiknes, H. Ødegaard, H. Myklebust, *J. Membrane Sci.* **2004**, *242*, 47.
- [28] C. G. Guizard, A. C. Julbe, A. Ayrat, *J. Mater. Chem.* **1999**, *9*, 55.
- [29] a) B. E. Yoldas, *Amer.Ceram.Soc. Bull.* **1975**, *54*, 286. b) C. H. Chang, R. Gopalan, Y. S. Lin, *J. Membr. Sci.* **1994**, *91*, 27.

- [30] a) A. L. Linsebigler, G. Lu, J. T. Yates Jr., *Chem. Rev.* **1995**, 95, 735. b) S. U. M. Khan, M. Al-Shahry, W. B. Ingler, Jr., *Science* **2002**, 297, 2243.



## **Experimental**

Preparation of membranes with a top-layer of hierarchical LROF structure were performed over alumina disks with a diameter of 30 mm and thickness of 2 mm. 0.2 wt% of titanate nanofiber suspensions dispersed by ethanol dropped on the substrates, which were fixed on the chuck of a spin-coat processor. The coating was applied at the spinning velocity of 1000 r/min for 2 min. About 0.5 mL of the fiber suspension was used for each coating. The spin-coating process was repeated twice, followed by drying in air at 393 K, calcination at 773 K for 4 h. The heating rate is 1 K/min, starting from 393 K. Similarly, the 0.2 wt% of boehmite nanofiber suspension was applied on a calcined membrane with the layer of randomly oriented titanate nanofibers.

The membranes were mounted on a filtration set-up to assess their separation efficiency. The 10 wt % dispersion of the Latex spheres was diluted to 0.01 wt% with water. 30 mL of the dilution was used to test permeation passing through a prepared membrane. A pressure difference between the pressures on the feeding fluid and on the permeate was maintained stably at 20 kPa by a vacuum system to drive the filtration. The time taken for filtrating every 5 mL of fluid by the membrane under test was recorded. The fluids before and after filtration by the membrane were sampled for analysis. SEM images were collected on an SEM (FEI Quanta 200). The samples are coated by gold using BioRad SC500 sputter coater. The specimens from a liquid sample were prepared by dropping 5  $\mu$ L of solution on a glass slide, which was then dried under vacuum conditions. A JEOL JSM 6400F Field Emission SEM was also used to obtain high resolution images. The efficiency of membrane separation could be estimated directly by comparing the numbers of latex spheres in images of the specimens taken before and

after membrane filtration. The morphology of the nanofibers was recorded on a Philips CM200 Transmission Electron Microscope. UV-visible spectroscopy (UV-vis) on a Cary100 (Varian Inc.) spectrophotometer was also utilized to analyze the concentration change of the fluids before and after the filtration. The intensity of the adsorption band at 205 nm was adopted to determine the concentration using a standard plotting curve.

## Supporting information

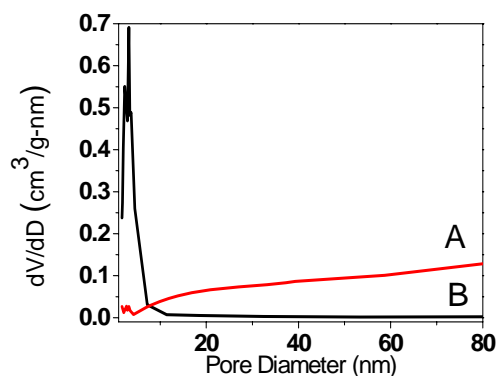


Fig. S1 Pore size distributions of the membrane with the LROF structure (A), calculated from the adsorption branch of the isotherm using BJH method. The PSD of the membranes of  $\gamma$ -alumina prepared by conventional method (B) is also given for comparison.

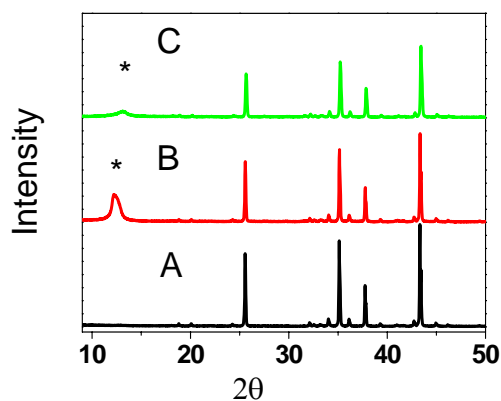


Fig. S2. XRD patterns of the LROF structure. (A)  $\alpha$ -alumina substrate, (B) the membrane after the three coatings of titanate fibers, and (C) the LROF membrane surface after three coatings of  $\gamma$ -alumina fibers on the top of the three coatings of titanate fibers. The diffraction

peak of titanate (labelled with \*) decreased after coating by the alumina fibers.